Amino Acids (2009) 36:185–193
DOI 10.1007/s00726-008-0046-5

ORIGINAL ARTICLE

Synthesis, spectroscopic and structural elucidation of sympathomimetic amine, tyraminium dihydrogenphosphate

Tsonko M. Kolev · Bojidarka B. Koleva · Michael Spiteller · William S. Sheldrick · Heike Mayer-Figge

Received: 1 December 2007 / Accepted: 11 February 2008 / Published online: 4 March 2008

Abstract The synthesis, isolation, spectroscopic and structural elucidation of sympathomimetic amine, tyramine dihydrogenphosphate are of interest due to its biological activity and the establishing correlation between spectroscopic properties and structure. The complex approach for investigation included single crystal X-ray diffraction, new technique in linear-polarized IR-spectroscopy in solid state and quantum chemical calculations with a view to predict the electronic structure and vibrational data of interacting species in entitled compound, the correlation structure–spectroscopic properties as well as the influence of intermolecular interaction on IR-characteristic bands are carried out.

T. M. Kolev (✉)
Institute of Organic Chemistry,
Bulgarian Academy of Sciences,
Acad. G. Bonchev Str. build. 9, 1113 Sofia, Bulgaria
e-mail: kolev@orgchm.bas.bg

T. M. Kolev
Faculty of Chemistry, Department of Organic Chemistry,
Plovdiv University "P. Hilendarski", 24 Tzar Assen Str,
4000 Plovdiv, Bulgaria

B. B. Koleva
Faculty of Chemistry, Department of Analytical Chemistry,
Sofia University "St. Kl. Ohridsky", 1164 Sofia, Bulgaria

M. Spiteller
Institut für Umweltforschung, Universitaet Dortmund,
Otto-Hahn-Strasse 6, 44221 Dortmund, Germany

W. S. Sheldrick · H. Mayer-Figge
Lehrstuhl für Analytische Chemie,
Ruhr-Universitaet Bochum, University Strasse 150,
44780 Bochum, Germany

Keywords Tyramine dihydrogenphosphate · Single crystal X-ray diffraction · Solid-state IR-LD spectroscopy · Quantum chemical calculations · Vibrational analysis

Introduction

Tyramine is a monoamine compound of 4-hydroxy phenethylamine and it is derived from tyrosine, an amino acid (protein building block), which is the precursor of norepinephrine. It, through its effect on neurotransmitters, may affect several health conditions including Parkinson's disease, depression, alcohol withdrawal support, and phenylketonuria. Tyramine or its derivatives can be used in pharmaceutical industry as sympathomimetic or adrenergic drugs themselves or as their intermediates; intermediate for bezafibrate used in the treatment of high cholesterol levels, for determination of peroxide activity in the fluorescence enzyme immunoassay for insulin or false transmitters, etc. In the living cell, the neurotransmitters acted in protonated form. Their ingestion would normally have no significant cardiovascular effects, but hypertensive crisis can occur in patients taking monoamine oxidase inhibitors. This phenomenon inspired many researchers to investigate the effects of tyramine on the cardiovascular system (Simon 2000). Tyramine has been widely used to understand the physiology and the pathophysiology of the autonomic nervous system regulating the cardiovascular system. This approach seems to be valid when tyramine is infused directly into a vascular bed, e.g. the forearm or the coronary circulation; intra-arterial infusion of tyramine at doses devoid of systemic effects causes a significant increase in local norepinephrine release and a corresponding vasoconstriction (Jacob et al. 2003; Abouzaglou et al. 2004).

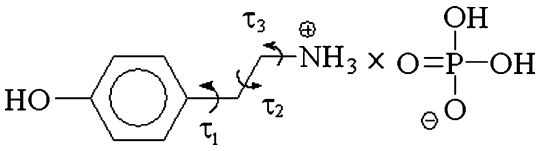

Scheme 1 Chemical diagram of tyramine dihydrogenphosphate

Surprisingly, the spectroscopic and structural elucidation of tyramine are less well characterized and only its hydrochloride has been characterized structurally. On the other hand, phosphates are an essential nutrient for all organisms used in the biosynthesis of diverse cellular components including nucleic acids, proteins, lipids and sugars. It is therefore essential for organisms to have evolved regulatory mechanisms for acquisition, storage and release of this molecule (Torriani-Gorini et al. 1994). It is known that cardiovascular events are the most frequent cause of death in the patients with chronic renal failure. Heterotopic calcification of blood vessel walls occurs frequently with advanced age, atherosclerosis and diabetes mellitus (Christian and Fitzpatrick 1999). In chronic renal failure, autopsy (Schwartz et al. 2000) and clinical investigations (Ikram et al. 1983) have documented a higher prevalence of coronary plaques in dialyzed patients when compared with non-uremic population. The risk factors that contribute to the higher prevalence of atherosclerotic lesions in chronic renal failure include hypophosphatemia, dyslipidemia, hyperhomocysteinemia and hypertension.

So, for the first time the synthesis, isolation, spectroscopic and structural elucidation of biological active tyraminium dihydrogenphosphate (Scheme 1) are reported. A tool for in vitro investigation with a view of describing the relationship of structure–spectroscopic properties giving a base for future in vivo studies is presented.

Experimental part

Synthesis

The title compound (tyraminium dihydrogenphosphate) was synthesized by adding methanol solution of tyramine (0.5671 g) and 1 M phosphoric acid (0.5 ml) with continuous stirring and heating. A colourless precipitate was obtained from the resulting solution after 30 min. The product was filtered off after cooling and recrystallized from methanol–acetonitrile (1:1) to afford the compound in quantitative yield. The purity of the compound was confirmed by IR and UV–Vis spectroscopy. Single prismatic and colourless crystals suitable for X-ray analysis were grown from methanol–acetonitrile (1:1) at room temperature over a period of the week (found: C, 40.88; H, 5.98; N, 5.96; $[C_8H_{14}NO_5P]$ calcd.: C, 40.86; H, 6.00; N, 5.96%). The most intensive signal in the mass spectrum is the peak at 138.24 m/z, corresponding to the singly charged cation $[C_8H_{12}NO]^+$ with a molecular weight of 138.19. The last data indicated, synonymously, the synthesis and isolation of entitled compound.

Materials and methods

Tyramine and phosphoric acid were purchased from Sigma-Aldrich and Merck, respectively. The X-ray diffraction intensities were measured in the ω scan mode on a Siemens P4 diffractometer equipped with Mo K_α radiation ($\lambda = 0.71073$ Å, $\theta_{max} = 30°$). The structure was solved by direct methods with the displacement ellipsoids depicted (Sheldrick 1995) and refined against F (Jacob et al. 2003; Sheldrick (1997). An ORTEP plot illustrates the anion and cation structures at the 50% probability level. Relevant crystallographic structure data and refinement details are presented in Table 1, selected bond distances and angles in Table 2. The hydrogen atoms were constrained to calculated positions and refined using riding models in all the cases.

The IR-spectra were measured on a Thermo Nicolet FTIR spectrometer OMNIC (4,000–400 , 0.5 cm^{-1} resolution, 150 scans) equipped with a Perkin Elmer wire-grid

Table 1 Crystal data, data collection and refinement results for tyraminium dihydrogenphospate

Empirical formula	$C_8H_{14}NO_5P'$
Formula weight	235.17
Temperature (K)	293(2)
Wavelength (Å)	0.71073
Crystal system, space group	Monoclinic, *Pn*
Unit cell dimensions	$a = 6.2422$ (12) Å
	$b = 11.731$ (2) Å
	$c = 7.7462$ (15) Å
	$\beta = 109.06$ (3)°
Volume ($Å^3$)	536.13 (18)
Z	2
Calculated density ($Mg \times m^{-3}$)	1.457
Absorption coefficient (mm^{-1})	0.258
F(000)	248
Crystal size (mm)	0.35×0.3×0.25
θ range for data collection	$7.5 \leq \theta \leq 15.0$
Limiting indices	$-1 \leq h \leq 8, -1 \leq k \leq 16, -10 \leq l \leq 10$
Absorption correction	ψ scans
Maximum and minimum transmission	0.769524/0.937398
Data/restraints/parameters	1562/3/1498
Goodness of fit on F^2	1.011
Final *R* indices [$I > 2\sigma$ (*I*)]	$R1 = 0.0372$, $wR2 = 0.1024$
R indices (all data)	$R1 = 0.0394$, $wR2 = 0.1043$

Table 2 Selected bond lengths (Å) and angles (°) for tyraminium dihydrogenphosphate from crystallographic data

C1 O1 1.372(3)	O1 C1 C2 122.2(2)
C1 C2 1.386(4)	O1 C1 C4 118.1(2)
C1 C4 1.389(4)	C2 C1 C4 119.6(2)
C2 C3 1.397(4)	C1 C2 C3 119.7(3)
C3 C6 1.389(4)	C6 C3 C2 121.9(3)
C4 C5 1.392(4)	C1 C4 C5 119.8(3)
C5 C6 1.396(5)	C6 C5 C4 121.7(3)
C6 C7 1.509(4)	C3 C6 C5 117.2(3)
C7 C8 1.511(4)	C3 C6 C7 121.1(3)
C8 N9 1.479(3)	C5 C6 C7 121.7(3)
P1′ O2′ 1.497(2)	C8 C7 C6 112.5(3)
P1′ O1′ 1.516(2)	N9 C8 C7 111.9(2)
P1′ O4′ 1.573(2)	O2′ P1′ O1′ 115.72(13)
P1′ O3′ 1.588(2)	O2′ P1′ O4′ 110.03(14)
	O1′ P1′ O4′ 107.07(14)
	O2′ P1′ O3′ 110.41(12)
	O1′ P1′ O3′ 108.21(13)
	O4′ P1′ O3′ 104.80(12)
O1 C1 C2 C3 −177.6(3)	C2 C3 C6 C7 179.6(3)
C4 C1 C2 C3 −0.1(5)	C4 C5 C6 C3 −0.9(6)
C1 C2 C3 C6 −0.2(5)	C4 C5 C6 C7 −179.7(4)
O1 C1 C4 C5 177.5(4)	C3 C6 C7 C8 120.7(4)
C2 C1 C4 C5 −0.1(6)	C5 C6 C7 C8 −60.5(5)
C1 C4 C5 C6 0.6(7)	C6 C7 C8 N9 −176.2(3)
C2 C3 C6 C5 0.7(6)	

polarizer. Non-polarized solid state IR-spectra were recorded using the KBr disk technique. The oriented samples were obtained as a suspension in the nematic liquid crystal (MLC 6815, Merck) with the presence of an isolated nitrile stretching IR-band at about 2,230 cm^{-1} additionally serving as an orientation indicator. The validation of this new orientation solid-state method used in linear-dichroic infrared (IR-LD) spectroscopy, based on suspension in nematic liquid crystal for accuracy, precision and the influence of the liquid crystal medium on peak positions and integral absorbances of the guest molecule bands have been presented (Ivanova et al. 2004). Optimization of experimental conditions and an experimental design for quantitative evaluation of the impact of four input factors has been presented (Ivanova et al. 2006a; Ivanova et al. (2006b)The number of scans, the rubbing-out of KBr-pellets, the amount of studied compounds included in the liquid crystal medium and the ratios of Lorentzian to Gaussian peak functions in the curve -fitting procedure on the spectroscopic signal at five different frequencies have been studied (Ivanova et al. 2006a; Ivanova et al. 2006b). It has been found that the procedure for the position (v_i) and integral absorbancies (A_i) determination for each *i*-peak have been carried out by deconvolution and curve-fitting procedures at 50:50% ratio of Lorentzian to Gaussian peak functions, χ^2 factors within 0.00066–0.00019 (in our case) and 2,000 iterations (Ivanova et al. 2006a, b). The means of two treatments were compared by Student *t*-test. The experimental IR-spectral patterns have been acquired and processed by GRAMS/AI 7.01 IR-spectroscopy (Thermo Galactic, USA) and STATISTICA for Windows 5.0 (StatSoft, Inc., Tulsa, OK, USA) program packages. The applicability of the last approach for experimental IR-spectroscopic band assignment and for obtaining the stereo-structural information has been demonstrated in a series of organic systems and coordination complexes as heterocyclic (Ivanova 2005a), Cu(II) complexes (Ivanova 2005b), polymorphs (Ivanova and Mayer-Figge 2005), codeine derivatives (Ivanova 2005c), peptides their Au(III) complexes, hydrochlorides and hydrogensquarates (Koleva 2006a, b; Ivanova 2006a, b, c, d; Bakalska et al. 2006; Ivanova et al. 2006c). The theory of IR-LD spectroscopy and the employed polarized IR-spectra interpretation difference-reduction procedure are given in Koleva et al. (2006a, b, c), Koleva (2006c, d)

The FAB mass spectra were recorded on a Fisons VG autospect instrument employing 3-nitrobenzylalcohol as a matrix. The elemental analysis was carried out according to the standard procedures for C, H (as CO_2 and H_2O) and N (by Dumas method).

Quantum chemical calculations were performed with GAUSSIAN 98 program package (Frisch et al. 1998). The output fails are visualized by means of ChemCraft program (Zhurko and Zhurko 2005). The geometry of tyraminium dihydrogenphosphate system was optimized at two levels of theory: second-order Möller–Pleset perturbation theory (MP2) and density functional theory (DFT) using 6-311++G** basis set. DFT method employed is B3LYP, which combines Becke's three-parameter non-local exchange functional, with the correlation function of Lee, Yang and Parr (Backe 1993; Lee et al. 1988) is applied. Molecular geometry of the studied species was fully optimized by the force gradient method using Bernys' algorithm (Peng et al. 1996). For every structure the stationary points found on the molecule potential energy, hypersurphases were characterized using standard analytical harmonic vibrational analysis. The absence of the imaginary frequencies, as well the of negative eigenvalues of the second-derivative matrix, confirmed that the stationary points correspond to minima of the potential energy hypersurfaces. The calculation of vibrational frequencies and infrared intensities were checked the calculations, performed, that agree best with the experimental data. In our case the DFT method provide more accurate vibrational data, as far as the calculated standard deviations are 10 cm^{-1} (B3LYP) and 19 cm^{-1} (MP2), respectively. So, the B3LYP/6-311++G** data are presented for above discussed modes, where for the

Table 3 Calculated (B3LYP/6-311++G**) geometry parameters as bond lengths (Å) and angles (°) of interacting tyraminium cation and dihydrogenphosphate anion, using atom numbering Scheme 2

Name definition	Bond length (Å)	Name definition	Angle (°)
R(1,2)	1.403	*A*(2,1,7)	121.4 (4)
R(1,7)	1.416	*A*(1,2,3)	119.8 (0)
R(2,3)	1.422	*A*(2,3,4)	117.2 (1)
R(3,4)	1.412	*A*(2,3,5)	119.2 (9)
R(3,5)	1.421	*A*(4,3,5)	123.4 (8)
R(5,6)	1.404	*A*(3,5,6)	119.9 (2)
R(6,7)	1.414	*A*(5,6,7)	121.3 (1)
R(7,8)	1.540	*A*(1,7,6)	118.2 (1)
R(8,9)	1.575	*A*(1,7,8)	121.0 (3)
R(9,10)	1.507	*A*(6,7,8)	120.7 (2)
R(10,25)	2.521	*A*(7,8,9)	112.3 (5)
R(23,24)	1.553	*A*(8,9,10)	113.9 (2)
R(24,25)	1.692	*A*(8,9,18)	109.0 (6)
R(24,26)	1.831	*A*(23,24,25)	122.6 (9)
R(24,27)	1.760	*A*(23,24,26)	112.8 (1)
		A(25,24,27)	101.3 (8)
		A(26,24,27)	91.8 (2)
		A(10,25,24)	93.9 (8)
Dihedral angles [o]			
Name definition		Name definition	
D(7,1,2,3)	0.0	*D*(5,6,7,1)	0.1
D(2,1,7,6)	0.1	*D*(5,6,7,8)	178.5
D(2,1,7,8)	178.5	*D*(1,7,8,9)	97.9
D(1,2,3,4)	179.9	*D*(6,7,8,9)	80.4
D(1,2,3,5)	0.0	*D*(7,8,9,10)	61.2
D(2,3,5,6)	0.1	*D*(23,24,25,10)	124.7
D(4,3,5,6)	179.9	*D*(23,24,25,20)	123.2
D(3,5,6,7)	0.1	*D*(27,24,25,10)	102.4
		D(10,25,26,28)	103.6

better correspondence between the experimental and theoretical values, a modification of the results using the empirical scaling factor 0.9614 (Scott and Radom 1996) is made. The calculated geometry parameters are presented in Table 3. The vibrational analysis and experimental IR-spectroscopic characteritic bands are shown in Table 4.

Table 4 A total of 1,700–400 cm^{-1} theoretical and experimental solid-state IR-characteristic bands of tyraminium dihydrogenphosphate

Assignment	ν (cm^{-1})		Assignment	ν (cm^{-1})	
	Exp.	Th.		Exp.	Th.
$\delta^{as}{}_{N+H3}$	1,645	1,612	$\delta^{s}{}_{N+H3}$	1,515	1,500
$\delta^{as'}{}_{N+H3}$	1,615	1,600	**19a**	1,507	1,505
8a	1,600	1,600	**19b**	1,492	1,494
8b	1,546	1,548	**11-γ_{CH}**	823	823

The normal modes of benzene ring are noted using Wilson notation (Varsanyi 1969).

Result and discussion

Crystal structure

Compound studied crystallizes as monoclinic system and space group *Pn* (Fig. 1). The cation in crystal lattice possesses point group *Cs*. The moderate intermolecular hydrogen bonding $_{(cation)}HO\cdots O_{(anion)}$ 2.716, 2.665 Å, $_{(cation)}N^{+}H_3\cdots O_{(anion)}$ 3.008, 2.817, 2.752 Å forms a 3D network (Fig. 2). The structural parameters, i.e. bond lengths and angles correlated well with theoretical ones (Tables 2 and 3), thus confirming the applicability of the approximation method used.

Theoretical analysis

The gas phase calculations of interacting charged moieties (Scheme 2) shown a most stable conformer (E_{rel} = 0.7 kJ/mol) with τ_i (i = 1–3, Scheme 1) angles of 97.9°, 61.2° and 54.9°, respectively. Two intermolecular hydrogen bonds $N^{+}H_3\cdots O_{(anion)}$ are predicted with bond lengths of 2.511 Å and 2.521 Å (Scheme 2). Calculated geometry parameters as bond lengths and angles are listed in Table 3 and a good correlation with the crystallographic data is obtained due to the deviations between the data are less then 0.0570 Å and 0.2(5)°, respectively. The theoretical vibrational analysis predicts an IR-spectrum (Fig. 3; Table 4) with a highest frequency peak at 3,624 cm^{-1} corresponding to $\nu_{OH(cation)}$ and series of maxima at 3,533 and 3,528 cm^{-1}—ν_{OH} of hydrogenphosphate. The bands at 3,321, 3,310 and 3,245 cm^{-1} are assigned to symmetric and asymmetric stretching peaks of $N^{+}H_3$ group ($\nu^{as}{}_{N+H3}$, $\nu^{as}{}_{N+H3}$ and $\nu^{s}{}_{N+H3}$). In 3,100–3,000 are bands of in-plane modes of benzene. The 1,700–1,500 cm^{-1} region correspond to in-plane modes of benzene as well as of bending $N^{+}H_3$ ones. The typical for *p*-disubstituted benzene band of 11-γ_{CH} is at 823 cm^{-1} (see Table 4).

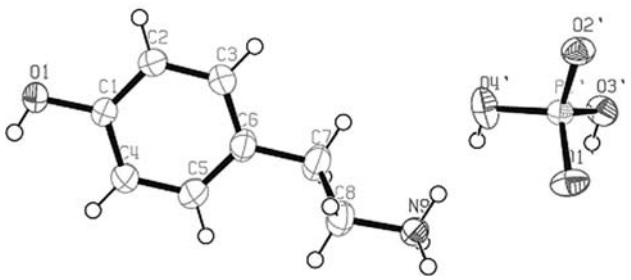

Fig. 1 ORTEP plot of tyraminium dihydrogen phosphate

Fig. 2 Unit cell and hydrogen bonding

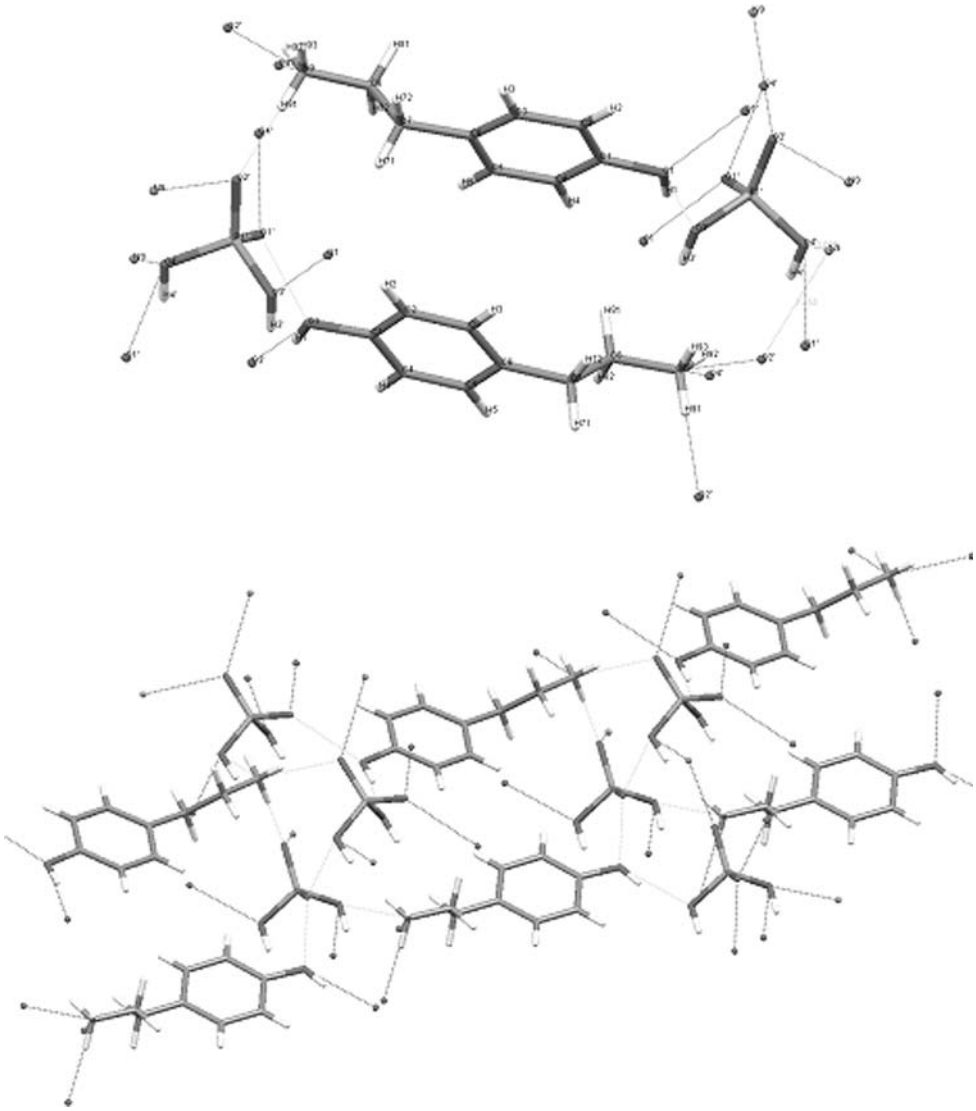

Scheme 2 Optimized conformer of interacting tyraminium cation and dihydrogenphosphate anion

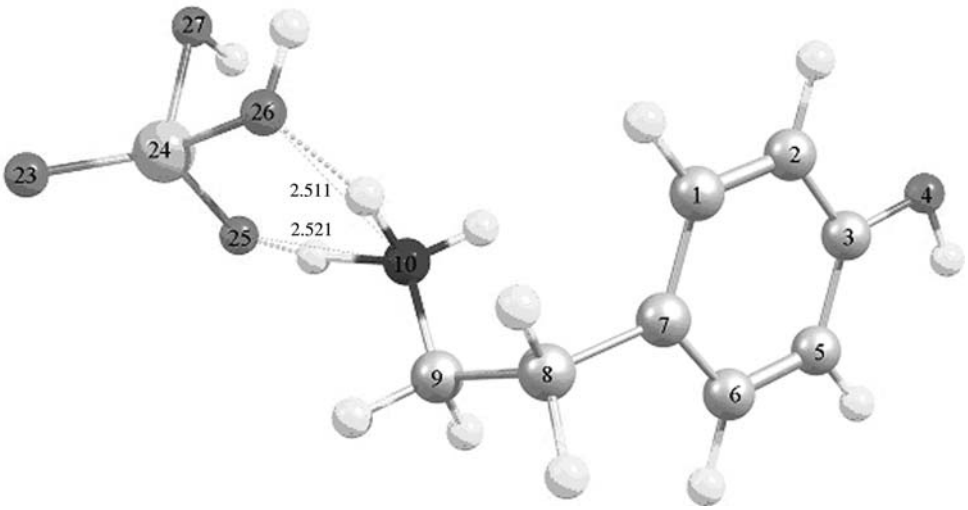

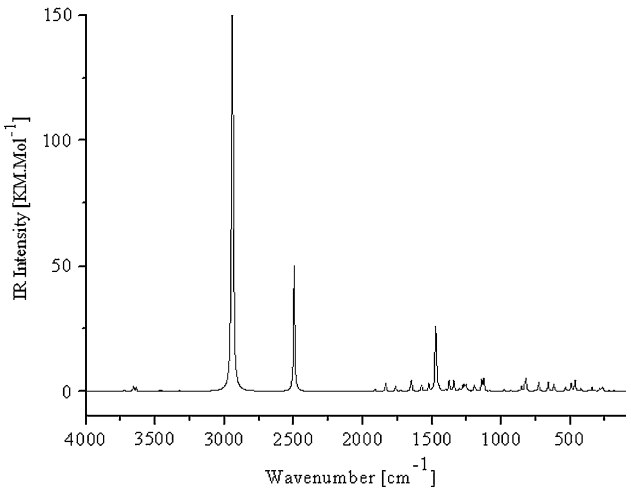

Fig. 3 Calculated IR-spectrum of tyraminium dihydrogenphosphate

Conventional and linear polarized IR-spectroscopic data

The experimental solid-state spectrum shows a broad maximum between 3,300 and 2,100 cm^{-1}. IR-spectroscopic region (Fig. 4) of the ν_{OH} stretching vibration in both cationic and anionic moieties, which overlapped the in-plane modes of benzene ring and the symmetric and asymmetric stretching ones. The characteristic maxima in 1,800–400 cm^{-1} range are presented in Table 4, by comparing with corresponding theoretical values. In all cases the interpretation of the spectral pattern requires a

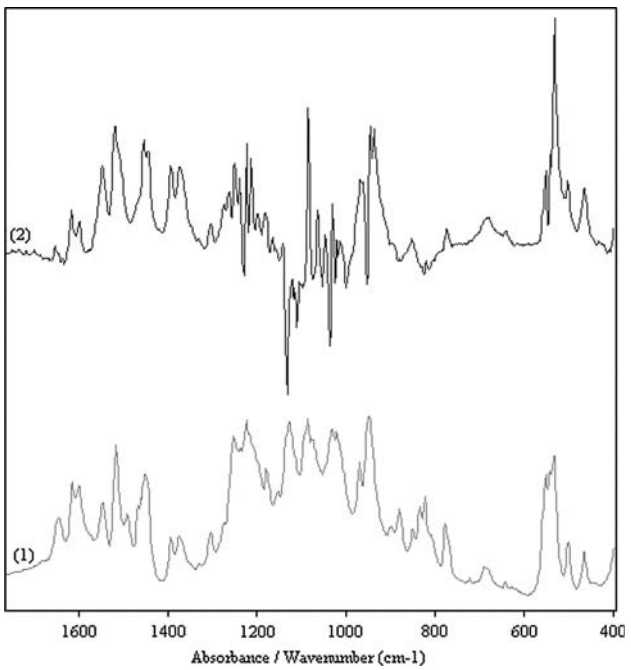

Fig. 4 Non-polarized IR (*1*) and difference IR-LD (*2*) spectrum of tyramide dyhydrogenphosphate

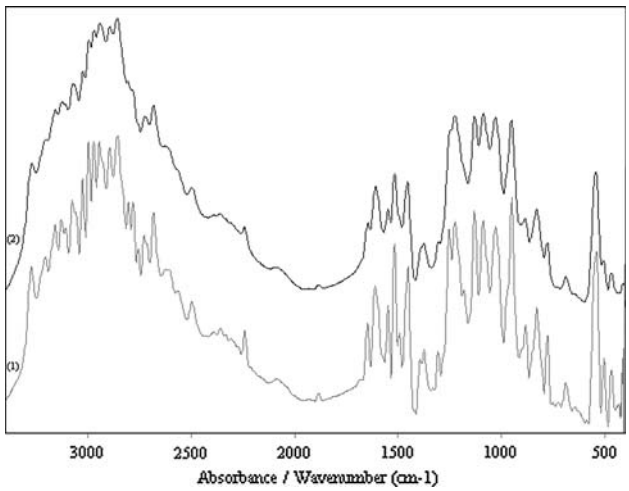

Fig. 5 Solid-state IR-spectrum of tyraminium dihudrogenphosphate: deconvoluted IR-spectral curve at γ factor 4.3 and increment 0.1 (*1*) and non-procedured IR-curve (*2*)

preliminary deconvolution and curve fitting procedures due to the complex and strong overlapped IR-spectrum of compound studied (Figs. 5, 6). The difference of less than 33 cm^{-1} between theoretical and experimental values obtained for banding vibration of NH_3^+ ($\delta^{as}{}_{N+H3}$, $\delta^{as'}{}_{N+H3}$, $\delta^{s}{}_{N+H3}$), due to the participation of this fragment in intermolecular interaction. For benzene modes, where the

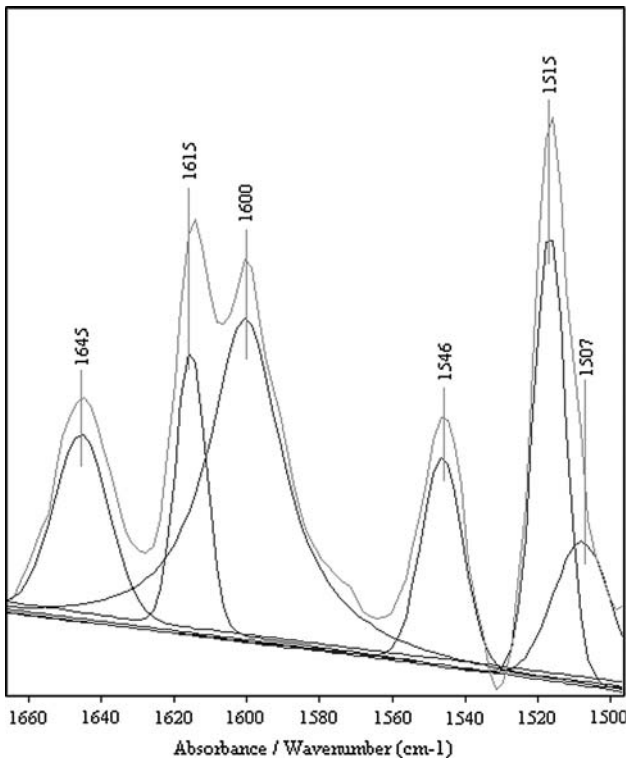

Fig. 6 Curve-fitted solid-state IR-spectrum of tyraminium dihudrogenphosphate

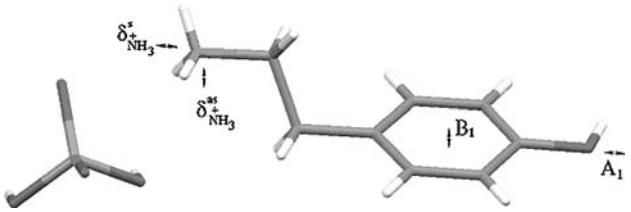

Scheme 3 Asymmetric unit of tyraminium dihydrogenphosphate

fragment does not influence the last interactions a difference of less than 3 cm^{-1} is obtained (Fig. 3) also confirming the assignment and predicted geometry (Scheme 3). Due to the frame of the unit cell co-linearity of δ^{s}_{N+H3} and A_1, in-plane modes of benzene are obtained. The elimination of these maxima at 1,600, 1,507 and 1,515 cm^{-1} (Table 4; Fig. 7; Scheme 4) in same dichroic cation confirms their origin and experimental geometry. The deviation of the τ_2 with 114.9° is a result of different types of intermolecular interaction in solid state, phenomenon typical for other amino acid amides and peptides (Koleva 2006a; Ivanova 2006a; Koleva 2006b; Ivanova 2005d; Bakalska et al. 2006; Ivanova 2006b; Ivanova 2006c; Ivanova et al. 2006c). On the other hand, the elimination of 823 cm^{-1} peak resulted in the disappearance of 1,645 and 1,615 cm^{-1}, which correlated with the experimental structure obtained and vibrational assignment (Fig. 8; Scheme 4).

In conclusion, it could be drawn that the structural and spectroscopic elucidation of sympaticomimetic tyraminium dihydrogenphosphate is presented with a view to explained the in vitro structure–spectroscopic properties on the basis of single crystal X-ray diffraction, solid-state liner polarized IR-spectroscopy and quantum chemical DFT calculation for obtaining the electronic structure and vibrational data.

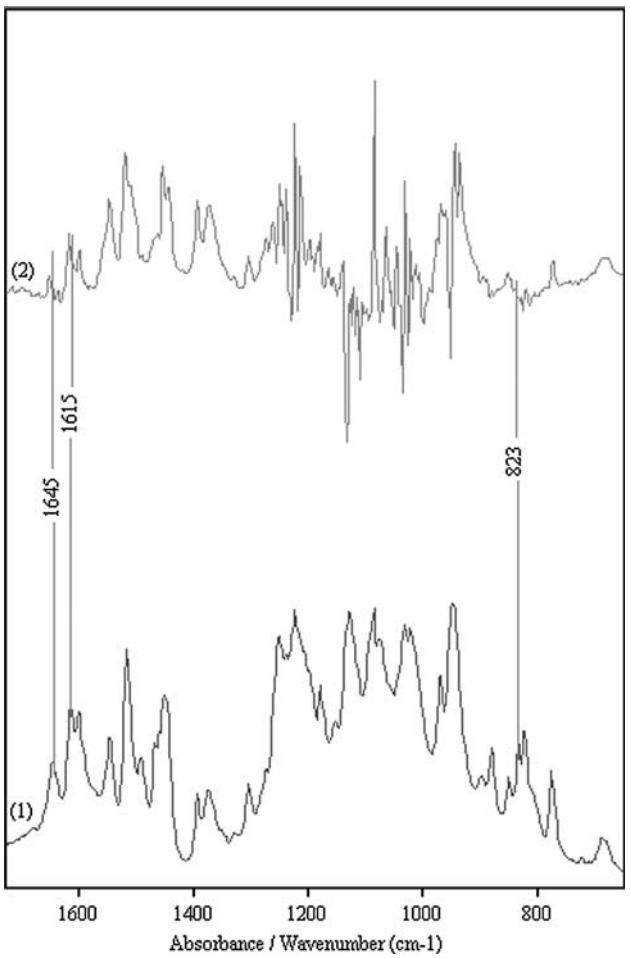

Fig. 7 Non-polaized IR (*1*) and reduced IR-LD (*2*) spectrum of tyraminium dihydrogenphosphate after elimination of 823 cm^{-1} peak

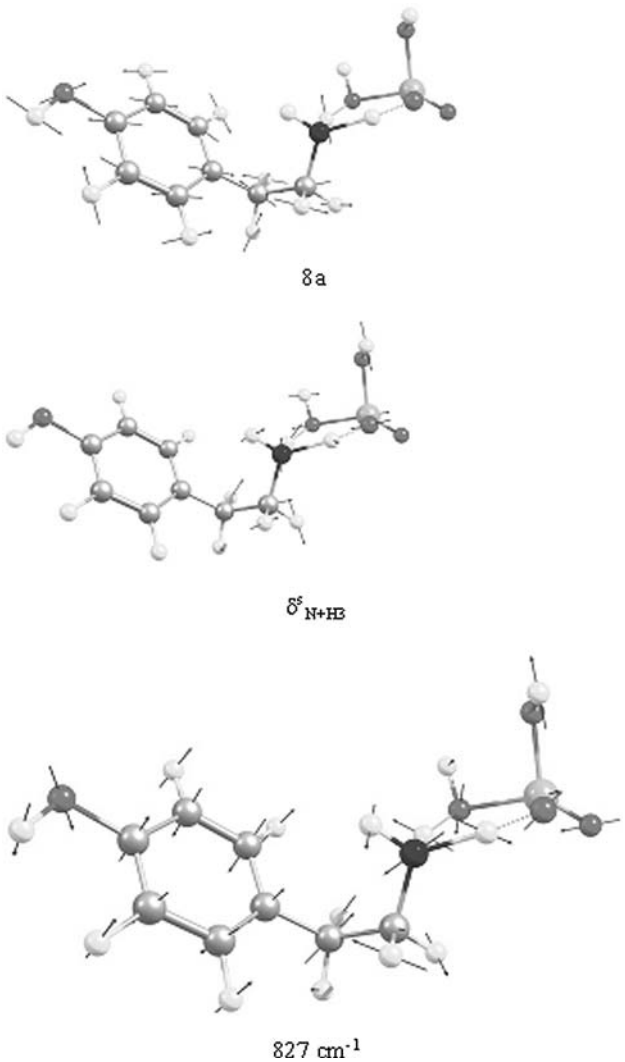

Scheme 4 Space direction of some transition moments

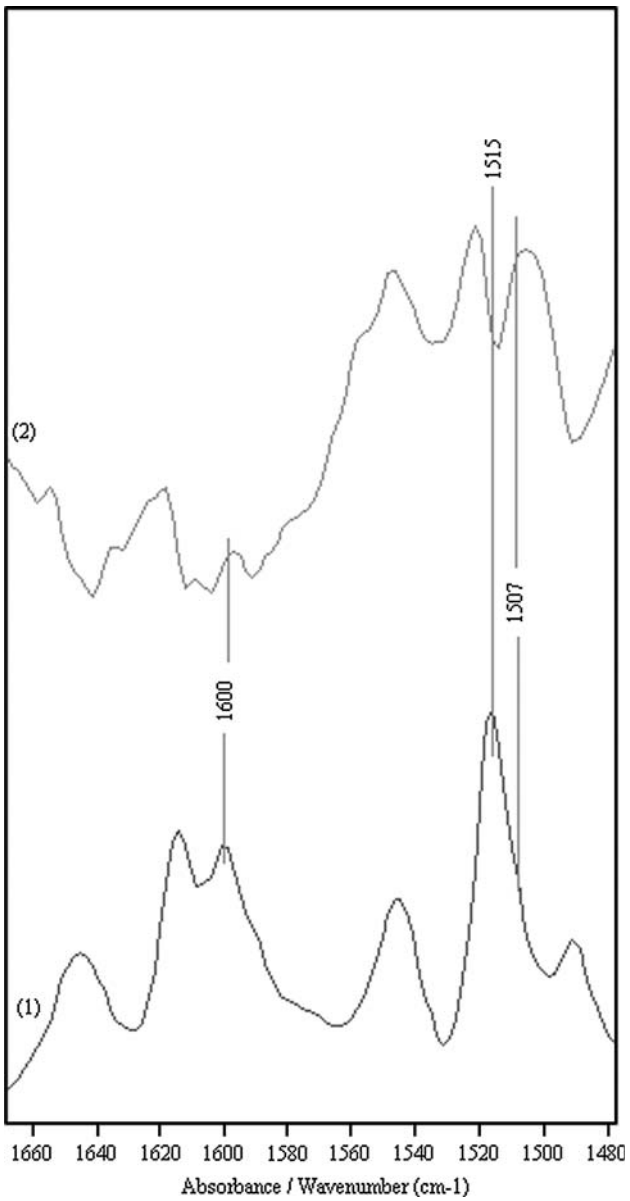

Fig. 8 Non-polaized IR (*1*) and reduced IR-LD (*2*) spectrum of tyraminium dihydrogenphosphate after elimination of 1,515 cm^{-1} peak

Acknowledgment T.K., B.K. and M.S. wish to thank the DAAD for a grant within the priority program "Stability Pact South-Eastern Europe" and the Alexander von Humboldt Foundation.

Appendix

Crystallographic data for the structural analysis have been deposited with the Cambridge Crystallographic Data Centre, CCDC 631838. Copies of this information may be obtained from the Director, CCDC, 12 Union Road, Cambridge, CB2 1EZ, UK (Fax: +44 1223 336 033; e-mail: deposit@ccdc.cam.ac.uk or http://www.ccdc.cam.ac.uk).

References

Abouzaglou J, Bé C, Gimona G, Roustan C, Kassab R, Fattoum A (2004) Eur J Biochem 271:2615–2623
Backe D (1993) J Chem Phys 98:5648
Bakalska R, Ivanova BB, Kolev Ts (2006) Cent Eur J Chem 4(3):533
Christian RC, Fitzpatrick LA (1999) Curr Opin Nephrol Hypertens 8:443–448
Frisch MJ, Trucks GW, Schlegel HB, Scuseria GE, Robb MA, Cheeseman JR, Zakrzewski VG, Montgomery JA Jr, Stratmann RE, Burant JC, Dapprich S, Millam JM, Daniels AD, Kudin KN, Strain MC, Farkas Ö, Tomasi J, Barone V, Cossi M, Cammi R, Mennucci B, Pomelli C, Adamo C, Clifford S, Ochterski J, Petersson GA, Ayala PY, Cui Q, Morokuma K, Salvador P, Dannenberg JJ, Malick DK, Rabuck AD, Raghavachari K, Foresman JB, Cioslowski J, Ortiz JV, Baboul AG, Stefanov BB, Liu G, Liashenko A, Piskorz P, Komáromi I, Gomperts R, Martin RL, Fox DJ, Keith T, Al-Laham MA, Peng CY, Nanayakkara A, Challacombe M, Gill PMW, Johnson B, Chen W, Wong MW, Andres JL, Gonzalez C, Head-Gordon M, Replogle ES, Pople JA (1998) Gaussian 98, Gaussian, Inc., Pittsburgh
Ivanova BB (2005a) Spectrosc Lett 38:635
Ivanova BB (2005b) Spectrochim Acta 62A:58
Ivanova BB (2005c) J Mol Struct 738:233
Ivanova BB (2005d) J Coord Chem 58(7):587
Ivanova BB (2006a) Cent Eur J Chem 4:111
Ivanova BB (2006b) J Mol Struct 782:122
Ivanova BB (2006c) Spectrochim Acta 64A:931
Ivanova BB, Mayer-Figge H (2005) J Coord Chem 58:653
Ivanova BB, Arnaudov MG, Bontchev PR (2004) Spectrochim Acta 60(4):855
Ivanova BB, Tsalev DL, Arnaudov MG (2006a) Talanta 69:822
Ivanova BB, Simeonov VD, Arnaudov MG, Tsalev DL (2006b) Spectrochim Acta Part A. (in press)
Ivanova BB, Kolev T, Zareva SY (2006c) Biopolymers 82:587
Ikram H, Lynn KL, Bailey RR, Little PJ (1983) Kidney Int 24: 371–376
Jacob G, Costa F, Vincent S, Robertson D (2003) Circulation 107. doi:10.1161/01.CIR.0000065605.37863.C0
Koleva BB (2006a) J Mol Struct. (in press)
Koleva BB (2006b) Vibr. Spectrosc. (in press)
Koleva BB (2006c) Spectrochim Acta, Part A. (in press)
Kolev Ts (2006d) Biopolymers 83:39
Koleva BB, Kolev Ts, Zareva SY, Spiteller M (2006a) J Mol Struct. (in press)
Kolev Ts, Zareva SY, Koleva BB, Spiteller M (2006b) Inorg Chim Acta. (in press)
Koleva BB, Kolev Ts, Spiteller M (2006c) Biopolymers. (in press)
Lee C, Yang W, Parr RG (1988) Phys Rev B37:785
Peng C, Ayala PY, Schlegel HB, Frisch MJ (1996) J Comp Chem 17:49
Sheldrick GM (1995) SHELXTL, Release 5.03 for Siemens R3 crystallographic research system. Siemens Analytical X-Ray Instruments, Inc., Madison, USA
Sheldrick GM (1997) SHELXS97 and SHELXL97. University of Goettingen, Germany
Scott AP, Radom L (1996) J Phys Chem 100:16502
Simon MA (2000) Cell 103:13–15

Schwartz U, Buzzello M, Ritz E, Stein G, Raabe G, Wiest G, Mall G, Amann K (2000) Nephrol Dial Transplant 15:218–223

Torriani-Gorini A, Silver S, Yagil E (1994) Phosphate in microorganisms: cellular and molecular biology. American Society for Microbiology, Washington D.C

Varsanyi G (1969) Vibrational spectra of benzene derivatives, Academy Press, Budapest, pp 1–413

Zhurko GA, Zhurko DA (2005) ChemCraft: Tool for treatment of chemical data, Lite version build 08 (freeware)